Vol. **108** (2005) *ACTA PHYSICA POLONICA A* No. 1

Proceedings of the XXI International Meeting on Radio and Microwave Spectroscopy
RAMIS 2005, Poznań-Będlewo, Poland, April 24–28, 2005

Electron Spin Relaxation of Cu(II) Ions in $ZnGeF_6 \cdot 6H_2O$ Crystal with Strong Jahn–Teller Effect

S. Idziak, S.K. Hoffmann* and J. Goslar

Institute of Molecular Physics, Polish Academy of Sciences
Smoluchowskiego 17, 60-179 Poznań, Poland

Cu^{2+} ions doped to $ZnGeF_6 \cdot 6H_2O$ substitute the host Zn^{2+} ions and undergo a strong Jahn–Teller effect producing nearly axial elongation of the $Cu(H_2O)_6$ octahedra with equal population of the three possible deformations at low temperatures as shown by the EPR spectra. Reorientations between these distorted configurations are observed as a continuous shift of EPR lines leading to averaging of the g- and A-tensors. The full averaging is observed at the phase transition temperature 200 K. Electron spin relaxation was measured up to 45 K only, where the electron spin echo signal was detectable. Electron spin–lattice relaxation is governed by the Raman two-phonon process allowing to determine the Debye temperature as $\Theta_D = 99$ K. There is no contribution of the Jahn–Teller dynamics to the spin–lattice relaxation rate. Electron spin echo decay is strongly modulated by dipolar coupling to the ^1H and ^{19}F nuclei. The phase memory time is governed by instantaneous diffusion at helium temperatures and then by spin–lattice relaxation processes and excitation to the first vibronic level of energy $\Delta = 151$ cm^{-1}.

PACS numbers: 63.90.+t, 76.30.–v

1. Introduction

Except the classical electron spin–lattice relaxation processes one can expect in some systems a contribution from other relaxation processes and mechanisms. One of them is the dynamics of the Jahn–Teller effect. Reorientations between the Jahn–Teller distorted configurations can be accompanied by spin flips producing recovery to the equilibrium population of spin levels. Although in the early

*corresponding author; e-mail: skh@ifmpan.poznan.pl

papers [1–3] it was claimed that a contribution from vibronic dynamics was identified in spin–lattice relaxation of some crystals containing vibronic $Cu(H_2O)_6$-ions, these results are not convincing since they were collected in a very low temperature range only and for samples with relatively high Cu^{2+} concentration (order of 0.01% or higher). The increase in sensitivity of modern pulsed EPR spectrometers allows currently to measure much shorter relaxation time T_1, thus to extend the experimental temperature range to higher temperatures.

In our previous electron spin echo (ESE) measurements of the electron spin relaxation in series of Cu^{2+} doped Tutton salts we clearly showed that the relaxation rate is determined by two-phonon Raman processes and is not influenced at all by the Jahn–Teller reorientations up to about 70 K where ESE signal disappears [4]. Moreover, we realized that the purity of samples used for ESE measurements has to be much higher than that used typically in cw-EPR experiments. Paramagnetic impurities, like Mn^{2+}, Fe^{3+}, or Cr^{3+} ions, even in concentration non-detectable clearly by cw-EPR spectra, can influence strongly ESE experiments by cross-relaxation. We found such a situation during our preliminary studies of $ZnSiF_6 \cdot 6H_2O$ doped with Cu^{2+} where we tried to verify the old ESE measurements [5]. We found that non-removable Mn^{2+} impurity in the crystal strongly influenced Cu^{2+} relaxation, making it impossible to measure the Cu^{2+} relaxation alone. We found, however, that it is possible to grow high purity single crystals of isostructural $ZnGeF_6 \cdot 6H_2O$ compound.

In this paper we present the results of ESE measurements of spin–lattice relaxation and phase relaxation (ESE dephasing) in the temperature range 4–45 K. The results clearly show that spin–lattice relaxation is governed by phonon processes [6] but not by the Jahn–Teller reorientations in contradiction to the previous paper [5]. On the other hand, we have found that vibronic dynamics gives contribution to the phase memory relaxation of Cu^{2+} in $ZnGeF_6 \cdot 6H_2O$.

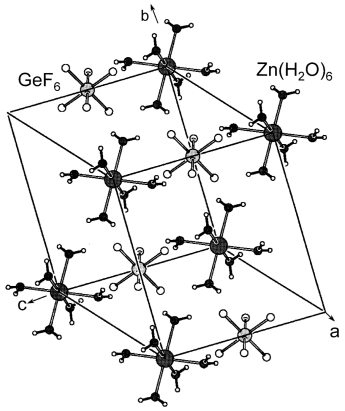

Fig. 1. Unit cell projection of $ZnGeF_6 \cdot 6H_2O$.

$ZnGeF_6{\cdot}6H_2O$ belongs to the family of isostructural fluosilicate hexahydrates having the CsCl-type structure composed of $Zn(H_2O)_6$ and GeF_6 octahedra in trigonal space group $R\bar{3}$ with hexagonal unit cell dimensions $a = 0.9363$ nm, $c = 0.9690$ nm, and $Z = 3$ for isostructural $ZnSiF_6{\cdot}6H_2O$ [7, 8] (Fig. 1). The water and fluorine octahedra are interconnected by hydrogen bonds and there exists a disorder of GeF_6 octahedra between two positions. Ordering of the octahedra leads to the first order phase transition at about 200 K in $ZnGeF_6 \cdot 6H_2O$ [9, 10] and at 272 K in $ZnZrF_6$ [11]. Copper(II) ions introduced in the host lattice of $ZnGeF_6 \cdot 6H_2O$ substitute Zn^{2+} ions and produce significant distortion of the nearly perfect O_h-symmetry water octahedra. This is due to strong Jahn–Teller effect leading to the three distortions of the water octahedra along Cu–O bonds separated by identical potential energy barriers of the order of 450–600 cm^{-1} [12]. An influence of the Jahn–Teller effect is visible in temperature dependence of the EPR spectrum as it will be shown in the next section.

2. Experimental

Single crystals were grown by slow evaporation of a water/HF solution of $ZnF_2 \cdot 4H_2O$ and GeO_2 at ambient temperature. Small amount of $CuF_2 \cdot 2H_2O$ was added to the mother solution with resulting Cu^{2+} concentration 3×10^{18}/g in the crystal as determined from EPR signal intensity.

Single crystal and powder EPR spectra were recorded in the frequency range 8.9–9.8 GHz and temperature range 4.2–45 K on a Radiopan SE/X-2547 and Bruker ESP 380E FT/CW spectrometer equipped with Oxford flow helium cryostats. The rotations of $ZnGeF_6{\cdot}6H_2O{:}Cu^{2+}$ single crystal allowed to determine the principal direction of the g-tensor (z-axis) and along this direction the ESE relaxation experiments were performed by exciting the $m_I = 1/2$ hyperfine line. Spin relaxation was measured with the Bruker ESP 380E FT/CW spectrometer.

Spin–lattice relaxation time was measured by the saturation recovery method using 24 ns saturating pulse and two 16 ns pulse sequence (with 144 ns interval) generating the Hahn echo. The monitored magnetization recovery was single exponential in the whole temperature range. The phase memory time T_M was determined from two-pulse Hahn echo amplitude decay strongly modulated by surrounding magnetic nuclei.

3. Results and discussion

3.1. EPR spectra and the Jahn–Teller effect

Single crystal EPR spectrum at room temperature consists of a single, isotropic, broad line. At low temperatures, in rigid limit below 50 K, the spectrum is composed of three hyperfine quartets indicating three chemically equivalent but differently oriented Cu^{2+} complexes (see spectrum (b) in Fig. 2). The g-factors

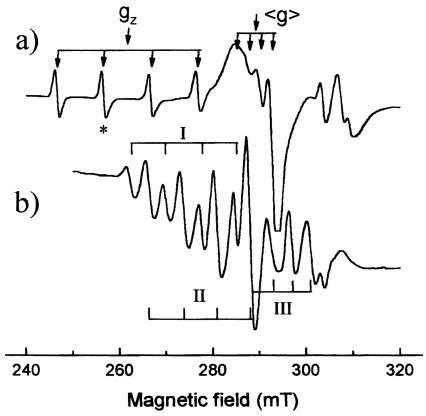

Fig. 2. Single crystal EPR spectra of Cu^{2+} in $ZnGeF_6 \cdot 6H_2O$ recorded at 50 K and at 8.9676 GHz: (a) along the g-factor z-axis (magnetic field parallel to the Cu–O bond). Pulsed ESE experiments were performed on the hyperfine line marked by the asterisk. The hyperfine quartet around the $\langle g \rangle$ arise from a trace of high temperature phase existing in the crystal after quenching; (b) along magnetic field direction deviated 60° from the z-axis. The three equivalent complexes are marked by I, II, and III.

TABLE

Spin-Hamiltonian and electron spin relaxation parameters of Cu^{2+} in $ZnGeF_6 \cdot 6H_2O$ single crystals (A-value in 10^{-4} cm^{-1}).

T [K]	g_z [a]	g_y	g_x	A_z [b]	A_y	A_x	Ref.
45	2.470	2.105	2.090	106	20		this paper
300	2.22			24			
4.2	2.472	2.103		–108.9	18.1		[13]
300	2.223						
4.2	2.473	2.103	2.095	104	20		[14]
Cu^{2+} in $ZnSiF_6 \cdot 6H_2O$							
4.2	2.460	2.100		107	14		[5]
77	2.22	2.23		21	29		

Spin–lattice relaxation rate: $1/T_1 = aT + bT^9 I_8(\Theta_D/T)$

$a = 0.1$ s^{-1} K^{-1} $\quad b = 1.2 \times 10^{-10}$ s^{-1} K^{-9} $\quad \Theta_D = 99$ K

Phase relaxation rate: $1/T_M = (1/T_M)_0 + 1/T_1 + c\exp(-\Delta/kT)$

$(1/T_M)_0 = 5 \times 10^5$ s^{-1} $\quad c = 2.5 \times 10^7$ s^{-1} $\quad \Delta = 151$ cm^{-1}

[a] Error in g-factors: ± 0.003. [b] Error in A-values: $\pm 3 \times 10^{-4}$ cm^{-1}.

are characteristic of elongated octahedral complexes of Cu^{2+} with ground state $d_{x^2-y^2}$. The principal g-factor and hyperfine splitting determined from rotational data at low temperatures are collected in Table, where they are compared with

the data of the other papers and with EPR data for Cu^{2+} in $ZnSiF_6 \cdot 6H_2O$. The principal g-factor axes are parallel to the Zn–O directions of the host $Zn(H_2O)_6$ octahedra. This proves that Cu^{2+} substitutes Zn^{2+} ions producing a strong deformation of the host water octahedra. This is due to the strong Jahn–Teller effect typical of Cu^{2+} in high symmetry octahedral environment as discussed in [13].

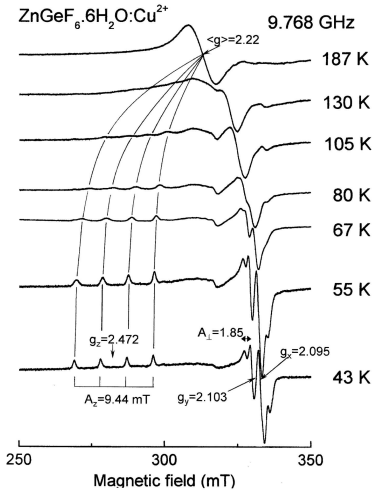

Fig. 3. Temperature variations of the EPR powder spectra showing vibronic shift of hyperfine lines along the z-axis.

The Jahn–Teller effect is essentially static below 50 K, whereas at higher temperatures the g-factor averaging is observed typical of vibronic averaging i.e. reorientations between three Jahn–Teller deformations of the $Cu(H_2O)_6$. It is well visible in powder EPR spectra presented in Fig. 3. At phase transition temperature about 200 K the full averaging of the spectrum takes place resulting in a single isotropic line at $\langle g \rangle$ [13]. The high temperature phase can be frozen in the low temperature phase by quenching of a crystal as it is indicated by EPR lines centred around $\langle g \rangle$ in Fig. 2a. Pulsed EPR experiments were performed along the z-axis on the hyperfine lines marked with asterisk in Fig. 2a where the isotope effect in the line width is the smallest.

3.2. Electron spin–lattice relaxation

Electron spin relaxation experiments were performed in the temperature range of 4.2–45 K only since at higher temperatures the ESE decay becomes so fast that the echo signal disappears in the dead time of the spectrometer. This indicates that initially homogeneously broadened EPR line becomes homogeneously broadened above 50 K. The recovery of magnetization after saturating pulse was single exponential in the whole temperature range as it is shown by the inset of Fig. 4. The spin–lattice relaxation rate $1/T_1$ increases with temperature as shown

in Fig. 4 and can be well described by the equation

$$\frac{1}{T_1} = aT + bT^9 \int_0^{\Theta_D/T} \frac{x^8 \exp(x)}{[\exp(x)-1]^2} \mathrm{d}x. \tag{1}$$

The second term which dominates the relaxation is due to the two-phonon Raman relaxation process for the Kramers ions with transport integral (called I_8) over the Debye-type phonon spectrum up to the Debye temperature Θ_D. The first term, linear in temperature, does not describe the direct relaxation process, but is rather due to phonon modes of energy Δ localized around lattice defects [15] and contributes considerably below 10 K only. This mechanism leads to the temperature dependence $1/T_1 \propto \mathrm{cosech}(\Delta/kT)$ which becomes linear for $kT > \Delta$. The best fit to Eq. (1) is shown as a solid line in $1/T_1$-plot of Fig. 4, with parameters: $a = 0.1\ \mathrm{s}^{-1}\ \mathrm{K}^{-1}$, $b = 1.2 \times 10^{-10}\ \mathrm{s}^{-1}\ \mathrm{K}^{-9}$, and the Debye temperature $\Theta_D = 99$ K.

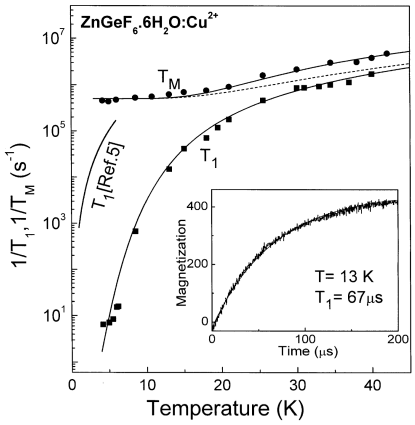

Fig. 4. Temperature variations of the spin–lattice relaxation rate $1/T_1$ and ESE dephasing rate $1/T_M$. The data of previous paper [5] are added as solid line in the low temperature range. The inset shows magnetization recovery after pulse excitation at 13 K with fitting to the single exponential function with $T_1 = 67$ μs.

Our results cannot be fitted with existing theories which predict that the Jahn–Teller effect dynamics should produce a contribution to the relaxation rate proportional to the Jahn–Teller reorientation rate which is proportional to T^5 or T^3 [16, 17]. The $1/T_1 \propto T^3$ was reported for Cu^{2+} in $ZnSiF_6 \cdot 6H_2O$, however, in a very narrow temperature range below 4 K limited by possibilities of the old pulse EPR technique [5]. The results of that paper are shown in Fig. 4 in a form of the solid line plotted for low temperatures, and indicate that the relaxation rate $1/T_1$ is about three orders of magnitude faster compared to our results. It is typical effect when concentration of Cu^{2+} is too high and interactions between Cu^{2+} ions are not negligible producing cross-relaxation, spectral and spin diffusion, and relaxation via copper-pairs or larger clusters. Thus, we conclude that in paper [5]

the pure relaxation processes were not observed and the T^3 dependence of the relaxation rate is accidental in narrow range of low temperatures.

3.3. Phase relaxation–electron spin echo dephasing

The two-pulse ESE amplitude V decreases when interpulse interval τ increases. The amplitude decay is strongly modulated as it is shown in Fig. 5a. Thus, effective decay function can be written as the product $V = V_{\mathrm{decay}} \cdot V_{\mathrm{mod}}$. The fitted decay function is shown as a solid line in Fig. 5a. After subtraction of the decay function and subsequent Fourier transform an ENDOR-like spectrum is obtained as shown in Fig. 5b. The spectrum contains peaks at proton Larmor frequency and at fluorine nuclear frequency indicating that many magnetic nuclei surrounding Cu^{2+} is involved in ESE modulations at this crystal orientation. The first harmonics at double frequency is also visible.

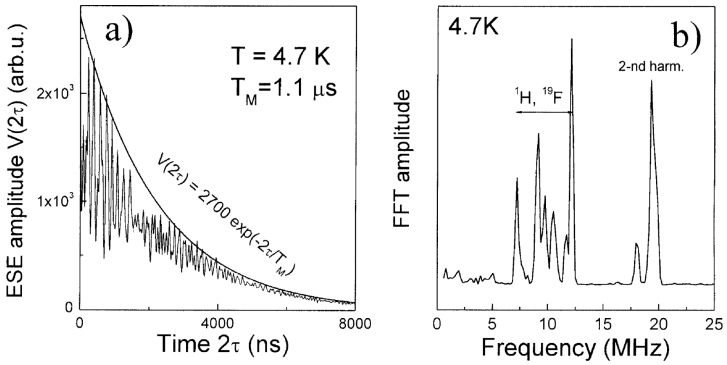

Fig. 5. (a) ESE decay recorded at 4.7 K strongly modulated by surrounding magnetic nuclei. The solid line is the exponential decay function. (b) FFT spectrum of the modulation function showing peaks at ^{1}H and ^{19}F nuclear frequencies and harmonic peaks at double frequencies.

The decay function was single exponential in the whole temperature range and described by: $V_{\mathrm{decay}} = V_0 \exp(-2\tau/T_{\mathrm{M}})$ where T_{M} is the phase memory time. Such a decay function is characteristic of instantaneous diffusion produced by second pulse and of molecular motions. A contribution type $\exp(-m\tau^2)$ to the decay has not been observed, indicating that both the electron and nuclear spectral diffusions are negligible [18]. The ESE dephasing rate $1/T_{\mathrm{M}}$ grows weakly with temperature as shown in Fig. 4. Such a behaviour has been observed in many copper(II) complexes [19, 20] and due to a contribution from spin–lattice relaxation processes. In fact, the spin–lattice relaxation rate $1/T_1$ approaches the $1/T_{\mathrm{M}}$ above 20 K as visible in Fig. 4. Thus, a contribution from T_1-type processes to ESE decay is expected but we have found that it is not enough to explain the observed increase in the dephasing rate with temperature. We have fitted the $1/T_{\mathrm{M}}$

rate to the equation

$$\frac{1}{T_{\mathrm{M}}} = \left(\frac{1}{T_{\mathrm{M}}}\right)_0 + \frac{1}{T_1} + c\exp\left(-\frac{\Delta}{kT}\right) \tag{2}$$

with parameters $(1/T_{\mathrm{M}})_0 = 5\times10^5$ s^{-1}, $c = 2.5\times10^7$ s^{-1}, $\Delta = 105$ K $= 151$ cm^{-1} and $1/T_1$ as in Eq. (1). The first term in Eq. (2) describes temperature independent contribution arising from the instantaneous diffusion. The exponential term appears generally in the Jahn–Teller systems [4, 17, 21] and describes contribution from excitations to higher vibronic levels. The Δ-value is typical of energy of the vibronic levels in the Jahn–Teller systems. Excitations to the pure vibrational levels do not influence spin dephasing but such an influence is possible via vibronic levels. In vibronic wave function the vibrational and electronic contributions are mixed and excitations between vibronic levels can produce random precession phase in the way similar to the T_1-processes. Thus, Δ can be considered as energy of the first excited vibronic state in the deepest potential well.

4. Conclusions

Fluosilicates doped with Cu^{2+} were considered for a long time as model crystals where the Jahn–Teller effect dynamics is the major mechanism of the electron spin–lattice relaxation. This was based on experimental data collected 30 years ago for Cu^{2+} in $ZnSiF_6\cdot 6H_2O$ [5]. Our results are in clear contradiction to those results (collected below 4 K) and indicate that the Jahn–Teller effect does not contribute to the spin–lattice relaxation up to 40 K. Thus, our general conclusion is that in all crystals we have studied so far the Jahn–Teller dynamics does not contribute to the spin–lattice relaxation which is governed by ordinary two-phonon processes. An influence of the Jahn–Teller effect is visible, however, as a contribution to the temperature dependence of the ESE dephasing rate. This is due to transitions between vibronic levels producing randomization of the phase of the spin precession motion. This is a new, specific for the Jahn–Teller systems, mechanism of the phase relaxation giving a possibility to determine the energy Δ of the first excited vibronic level of a system.

Acknowledgments

Authors thank to Dr. Maria Augustyniak-Jabłokow for supply of the crystals.

References

[1] K.P. Lee, D. Walsh, *Phys. Lett. B* **27**, 17 (1968).

[2] D.P. Breen, D.C. Krupka, F.I.B. Williams, *Phys. Rev.* **179**, 231 (1969).

[3] F.I.B. Williams, D.C. Krupka, D.P. Breen, *Phys. Rev.* **179**, 255 (1969).

[4] S.K. Hoffmann, J. Goslar, W. Hilczer, M.A. Augustyniak, M. Marciniak, *J. Phys. Chem. A* **102**, 1697 (1998).

[5] L.S. Dang, R. Buisson, F.I.B. Williams, *J. Phys. (France)* **35**, 49 (1974).

[6] S.K. Hoffmann, M.A. Augustyniak, J. Goslar, W. Hilczer, *Mol. Phys.* **95**, 1265 (1998).

[7] S. Ray, A. Zalkin, D.H. Templeton, *Acta Crystallogr. B* **29**, 2741 (1973).

[8] V.G. Kuznetsov, V.E. Gorbunova, E.F. Kovaleva, *Zh. Neorg. Khimii* **13**, 1309 (1969).

[9] Yu.V. Yablokov, M.M. Zaripov, A.M. Ziatdinov, R.L. Davidovich, *Chem. Phys. Lett.* **48**, 443 (1977).

[10] J. Grigas, R.L. Davidovich, A. Orlinkas, V. Samulionis, V. Skritskij, A. Urbanovitchius, *Krist. Technik* **15**, K72 (1980).

[11] V. Rodriguez, M. Couzi, A. Tressaut, J. Grannec, J.P. Chaminade, J.L. Soubeyroux, *J. Phys., Condens. Matter* **2**, 7373 (1990).

[12] M.A. Hitchman, W. Maaskant, J. van der Plas, C.J. Simmons, H. Stratemeier, *J. Am. Chem. Soc.* **121**, 1988 (1999).

[13] Yu.V. Yablokov, M.A. Augustyniak-Jablokov, M. Hitchman, D. Reinen, *Adv. Quantum Chem.* **44**, 483 (2003).

[14] S.N. Lukin, *Fiz. Tverd. Tela* **31**, 244 (1989).

[15] S.K. Hoffmann, W. Hilczer, J. Goslar, S. Kiczka, I. Polus, *Phys. Chem. Chem. Phys.* **4**, 4944 (2002).

[16] J.A. Sussmann, *J. Phys. Chem. Solids* **28**, 1643 (1967).

[17] F.S. Ham, in: *Electron Paramagnetic Resonance*, Ed. S. Geschwind, Plenum Press, New York 1972, Ch. 1.

[18] K.M. Salikhov, Yu.D. Tsvetkov, in: *Time Domain Electron Spin Resonance*, Eds. L. Kevan, R.N. Schwartz, Wiley, New York 1979, Ch. 7.

[19] S.K. Hoffmann, J. Goslar, W. Hilczer, M.A. Augustyniak-Jablokow, S. Kiczka, *J. Magn. Res.* **153**, 56 (2001).

[20] K. Nakagawa, M.B. Candelaria, W.W.C. Chink, S.S. Eaton, G.R. Eaton, *J. Magn. Res.* **98**, 81 (1992).

[21] S. Idziak, J. Goslar, S.K. Hoffmann, *Mol. Phys.* **102**, 55 (2004).